COMBUSTION AND FLAME 71: 41–50 (1988)

Determination of Absolute H Atom Concentrations in Low-Pressure Flames by Two-Photon Laser-Excited Fluorescence

J. BITTNER, K. KOHSE-HÖINGHAUS, U. MEIER, S. KELM and TH. JUST

DFVLR, Institut für Physikalische Chemie der Verbrennung, 7000 Stuttgart 80, W. Germany

A calibration technique is demonstrated which allows the determination of absolute atom concentrations in flames: two-photon laser-excited fluorescence signals from known atom concentrations generated in a discharge flow reactor are related to the fluorescence signals in a flame under identical excitation and detection conditions. With this method, absolute H atom profiles in several low-pressure hydrogen–oxygen flames have been obtained. For the same flame conditions, local temperature and absolute OH concentration profiles have been determined using laser-induced fluorescence (LIF). The experimental results are compared to the predictions of a one-dimensional flame model. The application of the new calibration technique to the atom detection in hydrocarbon flames is discussed.

1. INTRODUCTION

For comparison with chemical-kinetic flame models, the experimental determination of local concentrations of intermediate species in low-pressure flames is of considerable interest. Laser-induced fluorescence spectroscopy has been established as a valuable method for the investigation of such flames in terms of spatially resolved absolute radical concentration profiles and local temperatures. For the optical detection of the important atomic species, such as H and O in flames, multiphoton excitation techniques are required. Two- or three-photon induced fluorescence spectroscopy has been successfully employed for H [1–4] or O [5, 6] atom detection under different flame conditions. Alternative detection schemes were based upon resonant multiphoton ionization (MPI) for both H [7–9] and O [9, 10] atoms in flames. Apart from the fact that for fluorescence detection no probes have to be introduced into the flame as is the case for the MPI methods, it has the advantage that concentration mapping by imaging techniques is possible [11, 12]. Two major limitations have been reported. First, fluorescence detection schemes conventionally require shorter excitation wavelengths than the respective MPI schemes. The high UV power densities may cause considerable problems, as flame gases may be photolyzed to yield additional H or O atom concentrations not originally present in the flame [6, 13]. Second, the excited atoms are subject to quenching collisions which compete with the fluorescence. With respect to the locally different chemical composition of the flame, the fluorescence signal may thus depend on the effective quenching at the particular position in the flame. Attempts have been made to overcome these difficulties connected with multiphoton induced fluorescence detection of H and O atoms in flames by using preferably long excitation wavelengths to avoid photolysis effects [2, 3] and by circumventing the quenching effects by a special photoionization-controlled fluorescence detection scheme [1, 4].

With all the reported methods, relative atom concentration profiles in flames may be obtained, though precautions may be required in order to minimize the problems caused by laser photolysis, perturbation of the flame by ionization detectors, and locally different quenching. The quantitative detection of H and O atoms in flames, however, has only been attempted using an indirect calibra-

Published by Elsevier Science Publishing Co., Inc.
52 Vanderbilt Avenue, New York, NY 10017

0010-2180/88/$03.50

tion technique [9]. Recently we proposed a method which allows the determination of absolute concentration profiles of these atoms [14, 15]. The calibration is performed with the aid of a discharge flow reactor, where a known atom concentration is produced chemically. The fluorescence signals in both the flame and the flow reactor are compared under unchanged conditions for the two-photon excitation and fluorescence detection. Quenching and photolysis problems have been investigated in the chemically simple flow reactor system.

This paper reports the application of the new calibration technique to low-pressure hydrogen–oxygen flames, where absolute H atom concentrations could be determined.

2. EXPERIMENTAL

The experimental arrangement is shown in Ref. [14]. A detailed description of the conditions concerning the production of known atom concentrations in the discharge flow reactor, and of the parameters for the two-photon excitation and optical detection, has been given there. The thermostatted discharge flow reactor has been described earlier [16]. Details concerning the flat flame burner, the determination of absolute OH concentrations by saturated laser-induced fluorescence, and the measurement of local temperatures have also been reported elsewhere [17, 18]. A brief summary of the experimental procedure shall be given here.

The laser radiation for the excitation of H or OH was produced with an Nd : YAG laser pumped dye laser system (Quanta Ray) including a WEX frequency doubling and mixing unit and a Raman shifter. OH was excited in the A–X 0–0 band near 313 nm using frequency doubled radiation of a rhodamine dye mixture. The two-photon excitation of H atoms was performed with 205 nm radiation obtained by doubling the frequency of the output of a rhodamine dye mixture, mixing the resulting UV radiation with the rest of the IR beam, and additional Raman shifting in H_2. The laser power was monitored by a calibrated photodiode. Laser pulse energies of ≈ 1 mJ at 313 nm and ≤ 50 μJ at 205 nm were used for the respective excitation processes, corresponding to power densities of ≈ 300 MW/cm^2 and ≤ 70 MW/cm^2. In the case of OH, single line fluorescence was detected near 319 nm using a 0.6 m monochromator (Jobin Yvon) and a 1P28 photomultiplier (RCA). The H atom fluorescence was monitored near 656 nm through a suitable interference filter with a R928 photomultiplier (Hamamatsu). For both H and OH, the fluorescence signal was processed with a fast transient digitizer (Tektronix, resolution $\approx$ 1 ns) or a boxcar integrator (Stanford Research Systems) with a similar time resolution. Fluorescence signals were generally averaged for about 200 laser shots. The shot-to-shot fluctuations in laser intensity were less than $\pm 10\%$ at 313 nm and about $\pm 15\%$ at 205 nm. A PDP11/34 or PDP11/23 laboratory computer (Digital Equipment) was used for further evaluation of the data; additionally, it served for the control of several experimental parameters.

3. CALIBRATION PROCEDURE AND FLAME RESULTS

3.1 Physical Processes Involved in Quantitative H Atom Detection

For several reasons, the design of our quantitative H atom detection procedure requires the solution of the population differential equations of the atomic levels involved. First, it should be verified that the experimental conditions are suitable for a quantitative concentration measurement. Second, solutions of the equations with different collision terms make it possible to account for the different chemical environment in the flow reactor and in the flame experiment, and thus allow—under conditions discussed later—one to relate the respective fluorescence signals in the two systems to each other. Furthermore, the sensitivity of this calibration to such quantities as the two-photon absorption cross section or the photoionization rate, which may not be precisely known, is relevant for the accuracy of the concentration determination.

The processes for the H atom excitation and detection in our experiment are displayed schematically in Fig. 1. Two-photon excitation using laser radiation near 205 nm prepares a population in the

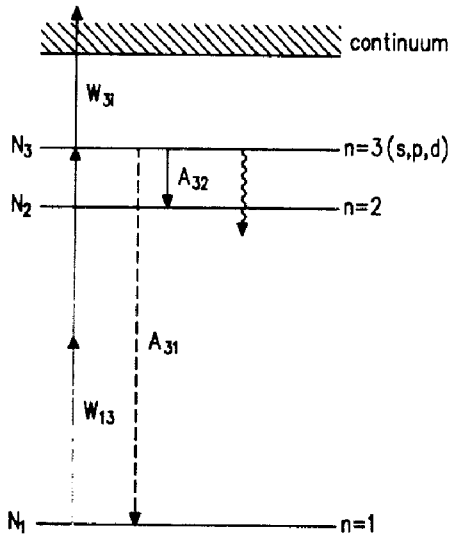

Fig. 1. Schematic energy level diagram for H atom excitation and detection: W_{13}, two-photon absorption rate coefficient; W_{3i}, photoionization rate coefficient; A_{31}, A_{32}, Einstein coefficients for spontaneous emission; N_1, N_2, N_3, populations in levels 1, 2, 3; serpentine line, collisional quenching processes.

$n = 3$ level of the H atom. The temporal evolution of this population N_3 may be described by the differential equation

$$\frac{dN_3}{dt} = N_1 \cdot W_{13} - N_3 \cdot (A_{31} + A_{32}) - N_3 \cdot W_{3i} - N_3 \cdot \sum_i k_i^T \cdot [M_i]. \quad (1)$$

In this equation, stimulated emission of the two-photon transition is neglected. $N_1 \cdot W_{13}$ is the two-photon excitation rate, A_{31} and A_{32} are the Einstein coefficients for spontaneous emission to levels 1 and 2, respectively, and $N_3 \cdot W_{3i}$ is the photoionization rate for ionizing transitions from $n = 3$. The effective collisional quenching rate for a specific gas mixture at the temperature T is given by the expression $N_3 \cdot \Sigma_i k_i^T \cdot [M_i]$, which is evaluated from the individual quenching rate coefficients k_i^T and the individual quencher concentrations $[M_i]$ at that temperature. The values of the different quantities which we use for the numerical solution of Eq. (1) shall be briefly discussed in the following.

The two-photon excitation rate coefficient W_{13} is given by [1]

$$W_{13} = \alpha_{13} \cdot I_L^2/h \cdot \nu_L, \quad (2)$$

where α_{13} is the two-photon absorption cross section, I_L the laser power density, and ν_L the frequency of the laser radiation; h is Planck's constant. A value for α_{13} is given by Bischel et al. [19]. For conditions similar to our experiment, it has been stated that the two-photon excitation in the 1s–3d transition is favored over the 1s–3s excitation [1, 20]. Due to the extremely small splitting of the fine structure components and the limited resolution of our experiment, we cannot observe whether a rapid collisional mixing of the 3s, p, and d states occurs. The measured average lifetime of (21.5 ± 1.5) ns [14], which was determined from a number of experiments under different conditions, indicates that the populations in the three sublevels do not immediately equilibrate. For the limited case of instantaneous mixing, a lifetime of the $n = 3$ state of 10 ns would be expected [21] due to the combined decay rates of the ($n = 3$)–($n = 2$) and ($n = 3$)–($n = 1$) transitions; the latter would be possible only if the 3p state would be populated. Our measured lifetime of 21.5 ns is consistent with the preservation of the initially prepared populations in 3s and 3d under the assumption of predominant 1s–3d excitation. For the numerical evaluation of Eq. (1), we approximate A_{32} be the inverse measured lifetime, which gives the effective radiative decay rate for our experiment.

The temporal shape of the laser pulse is approximated by

$$I_L = a \cdot t^b \cdot e^{-ct}, \quad (3)$$

where a, b, and c are constants obtained from fitting I_L to an average experimental laser pulse, with the restriction that the integral of I_L should be equal to the measured laser energy divided by the focal area.

Quenching rate coefficients for several collision partners (such as He, H_2, O_2, H_2O, and CH_4) have been determined in the discharge flow reactor; part of the measurements has been performed at elevated temperatures ($T \leq 700$K) [14]. For a given gas mixture at the temperature T, the effective quenching coefficient $\Sigma_i k_i^T \cdot [M_i]$ (in s^{-1}) can be evaluated, provided the individual quenching rate coefficients k_i^T (in $cm^3\ s^{-1}$) at the

temperature T and the quencher concentrations $[M_i]$ are known.

Three-photon resonant ionization may affect the quantitative fluorescence detection of H atoms. The photoionization rate coefficient for ionization out of the resonant $n = 3$ level, W_{3i}, can be defined as

$$W_{3i} = \sigma_{3i} \cdot I_L/h \cdot \nu_L. \quad (4)$$

The photoionization cross section σ_{3i} can be estimated by application of Kramers' formula [22] for the bound–continuum absorption coefficient of radiation with the frequency ν_L and the power density I_L absorbed by a hydrogen atom in the nth quantum state.

Model calculations with the system of differential equations for the energy levels of the H atom as described above showed that at the power densities used in our experiment, saturation or photoionization should not affect the quantitative fluorescence detection of H atoms. For a sensitivity test, we varied the two-photon absorption cross section, the laser power density, and the photoionization cross section independently by factors up to 10, considering different collisional quenching rates. In the limit of zero quenching, which corresponds approximately to the conditions in the flow reactor, the effect of the significant increase of the laser power density by a factor of 10 was hardly noticeable: a slight deviation from the square power dependence of the fluorescence signal on the laser power density was found. This result implies that the system is also insensitive to intensity fluctuations within the laser beam profile. Similar results were obtained when the photoionization cross section or the two-photon absorption cross section were increased by factors of 10. For effective quenching coefficients $\geq 10^9$ s^{-1}, as observed for flame conditions, the increase of any of these parameters did not affect the square power dependence; here, the collisional quenching is the dominant loss process out of the excited level, so that saturation and ionization are of limited influence.

We may conclude from this critical examination that a correct interpretation of fluorescence signals measured under our experimental conditions is possible even if we consider quite large uncertainties in the cross sections for two-photon absorption and photoionization. For the calibration it should be verified that the fluorescence intensity varies quadratically with the laser intensity, especially in the flow reactor system. The experiments should be performed at the lowest possible laser power density. This is also useful in view of the potential H atom production from H-containing compounds by the laser radiation, though we did not observe H atom fluorescence signals upon irradiation of large amounts of H_2 or H_2O in the flow reactor even for the highest available laser power densities [14]. Excitation and fluorescence detection of H atoms are accomplished on a nanosecond time scale, which is much shorter than the time constants for chemical reactions in the flame; this precludes interference by photodissociation of any other flame gases (like O_2), leading to perturbations in the chemical system.

3.2 Calibration

For the calculation of absolute H atom concentrations from measured two-photon excited fluorescence signals in flames without an external "standard" for the H atom concentration, several physical quantities must be known: the laser intensity and its spatial distribution, the two-photon absorption cross section, the rate coefficients for quenching, the detection geometry, and the efficiency of the optical detection system. A desired accuracy of the concentration measurement in the range of ± 20–30% implies that the error limits tolerable for individual parameters should be lower. This may not be trivial for such an experiment. Under conditions where the laser power density is low enough to avoid photoionization and to limit the influence of photodissociation, as discussed in the previous section, even the accurate determination of the power of the 205 nm laser pulse may cause difficulties: the readings of two calibrated UV-sensitive vacuum photodiodes (ITT F4000) and a surface absorbing disk calorimeter (Scientech 360001) differed by more than 20% at this wavelength. Similarly, the spatial laser intensity distribution in the focal volume is not easily obtained; it should, however, be known

with considerable accuracy because of the square dependence of the fluorescence signal on the laser intensity. An additional problem may be the accuracy of the two-photon absorption cross section.

From all these considerations, the use of an external atom concentration "standard," to which the fluorescence signal can be correlated, is preferable. When properly performed by interchanging only the burner and the flow reactor, keeping the laser running and all optical components untouched, our calibration method makes the determination of geometrical and optical parameters unnecessary. In our case, H atom concentrations in the flame can be evaluated from fluorescence signals using the relation

$$N_H{}^F = \frac{I_{Fl}{}^F}{I_{Fl}{}^R} \cdot N_H{}^R \cdot C_Q. \tag{5}$$

$N_H{}^F$ is the number density of H atoms in the flame, $N_H{}^R$ the known H number density in the flow reactor; $I_{Fl}{}^F$ and $I_{Fl}{}^R$ are the respective fluorescence signals in the two systems, measured with unchanged laser excitation and optical detection conditions. C_Q is a scaling factor.

The fluorescence intensity in the flow reactor results from a known H atom concentration, which is determined by titration with NO_2. This gives the absolute basis for the calibration. In contrast to the fluorescence signal in the flow reactor, the fluorescence intensity in the flame is strongly affected by quenching, so that for a correct comparison of the two signals, this loss factor has to be accounted for. The different collisional conditions influencing the fluorescence intensities in the two systems are considered by introducing the scaling factor C_Q. For a particular position in the flame, C_Q is evaluated by dividing the maximum population in the excited H atom level for the flow reactor conditions by the maximum population in this level obtained for the collisional conditions at this position in the flame. The populations are determined by solving the differential equations with the respective effective quenching coefficients.

The sensitivity of C_Q to changes in the two-photon absorption cross section, the photoionization cross section, and the laser power density was examined, using the same, considerable variations of these parameters as before, and found to be noticeable ($\geq 20\%$) for a slope of ≤ 1.8 in the logarithmic plot of the fluorescence intensity versus the laser power density. If a slope of close to 2.0 is obtained in the experiment, the systematic error in the calibration caused by uncertainties in the quantities addressed above is much less than 20%.

Laser-induced photodissociation of flame gases as a source of additional H atoms would cause a higher than square dependence of the fluorescence intensity on the laser intensity. The sensitivity of the slope in the logarithmic intensity diagram to the H production by the potential photodissociation processes and the associated changes in the population of the excited level is important for the estimation of systematic errors influencing our calibration. Recently, Goldsmith [13] reported that he created more H atoms than naturally present in his lean, atmospheric hydrogen–oxygen flame by his 205 nm laser pulse. The slope he obtained in the logarithmic intensity diagram in this case was 2.8, consistent with a cubic intensity dependence. With the cross section for the single photon dissociation of H_2O, most likely in a vibrationally excited state, which Goldsmith evaluated from his experiments, we estimated the influence of this process under our conditions. For this, we introduced an additional source term into the differential equation for the ground state. With this system of equations and the values of cross sections and quenching coefficients suitable for Goldsmith's flame conditions, we could well simulate his experimental observations. Both the population in the excited state and the power dependence are considerably sensitive to the ratio of vibrationally excited H_2O to naturally present H atoms. For our low-pressure hydrogen–oxygen flames, this ratio is at least a factor of 20 lower than in the flame of Goldsmith. Our calculations showed that this particular photodissociation process should not influence our concentration measurements, but that, if a slope of ≥ 2.2 would be measured, the change in the H atom concentration due to this process would be $\geq 50\%$. Photodissociation of ground state H_2O and H_2 has been investigated in the flow reactor [14] and should not

lead to erroneous H atom concentrations under our flame conditions.

3.3 Application of the Calibration Method to Hydrogen-Oxygen Flames

Three H_2-O_2-Ar flames at 95 mbar and equivalence ratios Φ of 0.6, 1.0, and 1.4 were investigated; their gas composition and maximum temperatures are shown in Table I. The flame conditions were chosen similar to those of Lucht et al [1, 23] and adapted to our burner diameter. We determined the local temperature profiles using rotational spectra of OH.

The dependence of the H atom fluorescence intensity on the laser intensity was measured for typical flow reactor conditions, as shown in Table IIa, and at various positions in the flames, including the one given in Table IIb. The laser intensity was varied using an optical attenuator adapted from Bennett and Byer [24] or suitable neutral density filters. The resulting logarithmic plots for these two conditions are displayed in Fig. 2. Within a typical accuracy of ± 5–10%, we did not observe any deviations from the expected quadratic behaviour either in the flow reactor or for the difference flame conditions.

The evaluation of absolute H atom concentrations from measured profiles of the fluorescence intensity in the three flames can thus be carried out as outlined above, using Eq. (5). The fluorescence intensity measured in the flow reactor corresponds to the H atom concentration determined by the titration with NO_2. The accuracy of a typical titration experiment, which, of course, limits the accuracy of the absolute concentration determination, is evident from Fig. 3. From the intersection with the abscissa, the H atom concentration is obtained which had been present before NO_2 addition, and which produces the fluorescence intensity given by the ordinate intercept. For this particular experiment, the linear correlation coef-

TABLE I

Gas Composition and Maximum Temperature of 95 mbar H_2-O_2-Ar Flames

Φ	H_2[cm³/min]	O_2[cm³/min]	Ar[cm³/min]	T[K]
0.6	485	405	1520	1350
1.0	714	357	1342	1350
1.4	894	319	1200	1100

TABLE II

Example of the Determination of the Scaling Factor C_Q

(a) Flow Reactor, H_2-He, 5.5 mbar

	H_2	He
Measured quenching rate coefficients k_i^T [10^{-9} cm³ s^{-1}] (Ref. [14])	2.2	No effect
Gas composition	1%	99%
Effective quenching coefficient $\Sigma_i k_i^T \cdot [M_i]$	$3 \cdot 10^6$ s^{-1}	

(b) H_2-O_2-Ar Flame, Φ = 0.6, 95 mbar, h = 3.5 mm

	H_2O	O_2	H_2	Ar
measured quenching rate coefficients k_i^T [10^{-9} cm³ s^{-1}] (Ref. [14])	11	2.6	2.2	0.46
Gas composition	15.5%	10.9%	2.0%	71.8%
Specific quenching coefficients $k_i^T \cdot [M_i]$ [10^8 s^{-1}]	10.8	1.79	0.28	2.09
Effective quenching coefficient $\Sigma_i k_i^T \cdot [M_i]$	$1.49 \cdot 10^9$ s^{-1}			
Scaling factor C_Q	4.35			

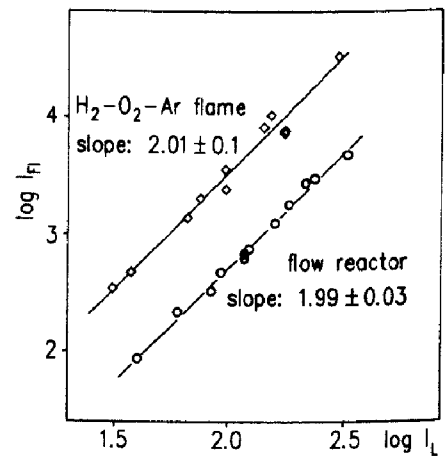

Fig. 2. Logarithmic plot of the H atom fluorescence intensity I_{Fl} versus the laser intensity I_L for the flow reactor and flame conditions of Table II.

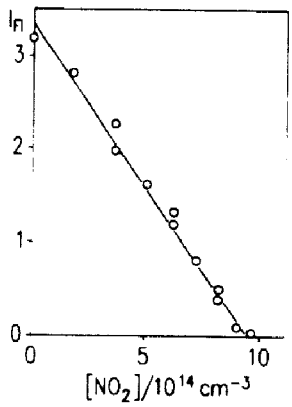

Fig. 3. Titration of H atoms with NO_2 in the flow reactor. The NO_2 sample for this experiment was 3.3% in helium as specified by the manufacturer (Messer Griesheim) and confirmed by chemical analysis in our laboratories. The fluorescence intensity (arbitrary units) and the NO_2 number density are correlated by a straight line with a linear correlation coefficient of 0.993. The laser intensity was constant for the titration.

ficient for the straight line is 0.993, corresponding to a standard deviation of the intercept of ±2.5%.

As an example for the evaluation of the scaling factor C_Q [Eq. (5)]. Table II lists the effective quenching coefficients for typical flow reactor conditions and for one particular position in the lean flame. The composition of the stable flame gases is taken from a simulation with a one-dimensional chemical-kinetic flame model [25]. Our measured temperature profile was used as input for the model. We regard the calculation of the stable gas composition as permissible under these flame conditions, where the mole fraction, in particular of the strong quencher H_2O, is only slightly dependent on temperature. Confidence in this method of evaluation is strongly supported by the fact that the absolute OH concentrations in the three flames, which are very sensitive to the input temperature profile, are well reproduced by the flame model.

Though the temperature-dependent quenching rate coefficients of the H atom by the major flame components were only determined in a limited temperature range (≤700K), we extrapolated them in a first approximation to the flame temperatures of 1000–1350K. The quenching rate coefficients, particularly for H_2O, exhibit only a negligible temperature dependence in the range of temperatures accessible in our flow reactor. The extremely fast quenching of the H atom fluorescence in a low-pressure flame is illustrated in Fig. 4. The time characteristics of the laser pulse and of the fluorescence signal in the lean H_2–O_2–Ar flame at 95 mbar, as measured with the photomultiplier, are displayed. No difference in the time behaviour is seen. For a comparison, under these flame conditions the inverse effective lifetime of OH ($A^2\Sigma^+$, $v = 0$) is $\approx 1.4 \cdot 10^8$ s^{-1}, which is about an order of magnitude lower than for H ($n = 3$) and which can easily be distinguished from the temporal shape of the laser pulse.

To obtain additional information on the effective quenching coefficient for the H atom under flame conditions, we decreased the flame pressure to 26 mbar, the lowest pressure which allowed us to stabilize the flame of this stoichiometry on our burner. For this pressure, the time decay of the fluorescence intensity was slightly slower than that of the laser pulse, so that an effective quenching coefficient could be extracted from this experiment, which was then compared with the one evaluated from the individual quenching rate coefficients and the flame gas composition. The procedure was as follows. In the first step, we had to determine how a fluorescence signal generated by a laser pulse with a known time behavior is transformed by the limited time response of the photomultiplier used. The time response of the photomultiplier was estimated from the temporal shape of individual dark current pulses. This

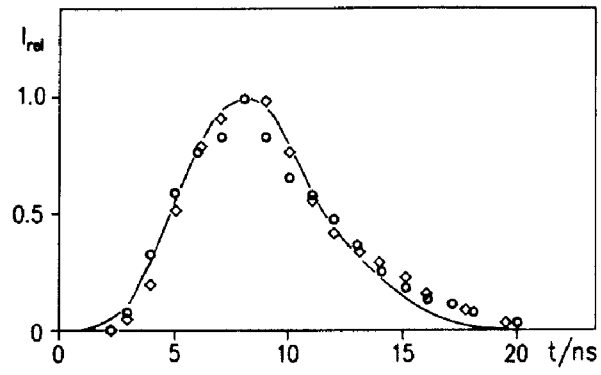

Fig. 4. Temporal shape of the laser pulse (○) and the fluorescence signal (◇) in the $\Phi = 0.6$ H_2–O_2–Ar flame at 95 mbar and $h = 3.5$ mm, both measured with a photomultiplier of limited time resolution. The solid line is obtained by convolution of the "real" time behavior of the laser pulse measured with a fast photodiode and the time response function of the photomultiplier.

procedure was validated by applying the response function to the well-known laser pulse. The convolution of the "real" average laser pulse measured with a fast photodiode with the response function of the photomultiplier resulted in the solid line in Fig. 4 in good agreement with the average laser pulse measured with the photomultiplier. The differential equation for the $n = 3$ level of the H atom was then solved with different effective quenching coefficients. Next, the resulting temporal shape of the fluorescence signal was convoluted with the time response function of the photomultiplier. Figure 5 shows the results. The measured time dependence of the fluorescence signal is best approximated by a calculation which considers an effective quenching coefficient on the order of $3 \cdot 10^8$ s^{-1}. From the individual quenching rate coefficients and the composition of the stable flame gases, which was calculated using the measured flame temperature, we obtained an effective quenching coefficient of $3.4 \cdot 10^8$ s^{-1} for this H_2–O_2–Ar flame at 26 mbar in excellent agreement with the calculated results of Fig. 5. This effective quenching coefficient is also in good qualitative agreement with a value of $3.1 \cdot 10^8$ s^{-1} reported by Lucht et al. [1] for a 26 mbar H_2–O_2–Ar flame of $\Phi = 1.4$. A better agreement cannot be expected considering the slightly different flame conditions which, unfortunately, are not completely reported for the flame of Lucht et al. The additional information provided by the measured time decay of the fluorescence intensity in the flame at 26 mbar confirms the validity of our extrapolation of the quenching rate coefficients to flame temperatures.

The local absolute concentration profiles of OH and H in the lean, stoichiometric, and rich H_2–O_2–Ar flames are displayed in Figs. 6–8 together with the calculation of these concentrations with our flame model. The algorithm was developed by Warnatz [25]. We introduced into the chemical submodel the most recent rate coefficients for the H_2/O_2 system. In particular, for the important reaction H + O_2 → OH + O the rate coefficient $k(T)$ of Frank and Just [26] was used. The statistical error limits for the OH concentration measurement are ±15% for the lean and stoichiometric flames and ±30% for the rich flame. For the H atom concentrations, the statistical error obtained from several calibration experiments is ±30%. Good agreement with the flame model calculations is found for the lean and stoichiometric flames regarding these error limits. The agreement of measured and calculated OH and H atom concentrations in the rich flame is satisfactory. A reason for this lesser accuracy in the concentrations may be the poorer accuracy attributable to the temperature profile, which was obtained from OH fluorescence spectra at comparatively low OH concentrations.

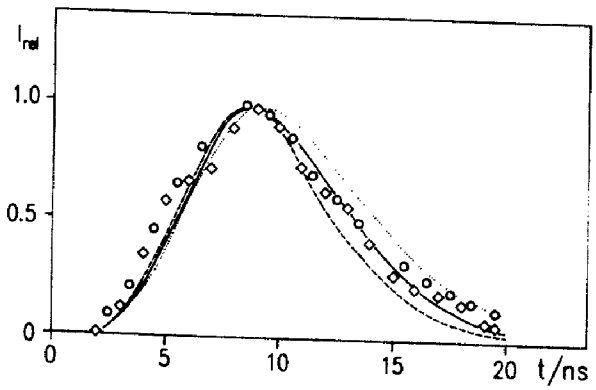

Fig. 5. Measured (○, ◇) and calculated temporal shape of the H atom fluorescence signal in a $\Phi = 0.6$ H_2–O_2–Ar flame at 26 mbar, considering the time response of the photomultiplier and different effective quenching coefficients in the calculations: ..., $2 \cdot 10^8$ s^{-1}; ——, $3 \cdot 10^8$ s^{-1}; – – –, $5 \cdot 10^8$ s^{-1}.

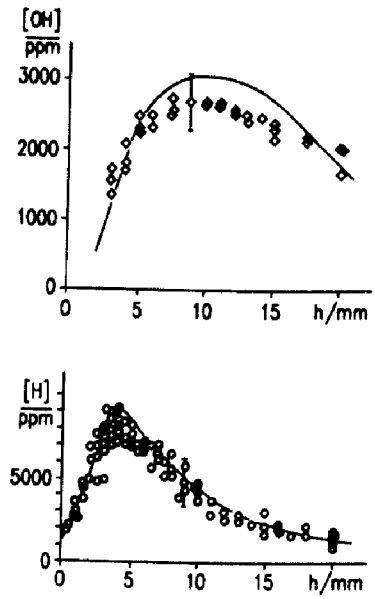

Fig. 6. Absolute OH (◇) and H (○) concentrations in an H_2–O_2–Ar flame at $\Phi = 0.6$ and 95 mbar. The solid lines represent the predictions of the flame model.

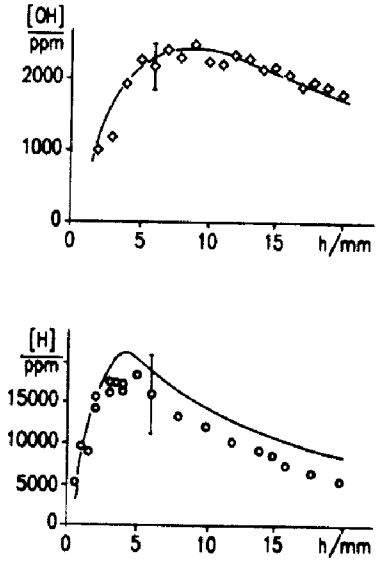

Fig. 7. Absolute OH (◇) and H (○) concentrations in an H_2-O_2-Ar flame at Φ = 1.0 and 95 mbar. The solid lines are the concentration profiles calculated with the flame model.

4. CONCLUSIONS

A calibration method for the determination of absolute H atom concentrations in flames was developed. The processes influencing the accuracy of the calibration were discussed in detail, especially with respect to photoionization and photodissociation. To avoid erroneous interpretation of the fluorescence signals, it is strongly recommended that one performs the calibration at the lowest possible laser power densities. The technique was applied to three H_2-O_2-Ar flames at different stoichiometries, for which we additionally measured absolute OH concentration profiles. The agreement of the measured OH and H atom concentrations with the predictions of a detailed chemical-kinetic flame model is good.

Preliminary experiments in hydrocarbon flames showed promising results. Though the number of chemical species is larger than in the hydrogen flames, the H atom concentration measurement is not affected by photodissociation processes under our conditions. For three different stoichiometries of low-pressure CH_4-O_2 flames at different positions above the burner surface, no deviations from a square dependence of the fluorescence intensity on the laser intensity was found. The number of quenchers is extended by species such as CO, CO_2, CH_4, and C_2H_2. The respective quenching rate coefficients at room temperature have been determined in the flow reactor. Profiles of the relative H atom concentrations for the three CH_4-O_2 flames agree well with the predictions of the flame model. In comparison with the concentration measurement in the H_2-O_2-Ar flames, the signal-to-noise ratio in the CH_4-O_2 flames and even more strongly in C_2H_2-O_2 flames is affected by flame emission in the wavelength range of 600-700 nm. Absolute concentration measurements in these flames will be performed in the near future following the procedure demonstrated for the H_2-O_2-Ar flames.

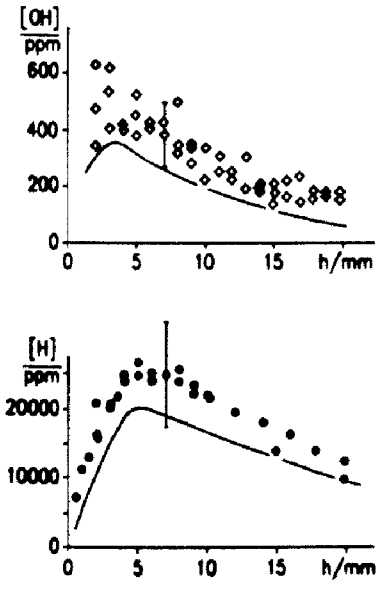

Fig. 8. Absolute OH (◇) and H (○) concentrations in an H_2-O_2-Ar flame at Φ = 1.4 and 95 mbar. The solid lines are the modeled concentrations.

This work was supported by the Stiftung Volkswagenwerk. The invaluable technical assistance of Peter Heberle and Hans-Peter Wenzler with constructive and electronic parts of the equipment is gratefully acknowledged. We thank Manfred Kapernaum for performing the NO_2 analysis.

REFERENCES

1. Lucht, R. P., Salmon, J. T., King, G. B., Sweeney, D. W., and Laurendeau, N. M., *Opt. Lett.* 8:365 (1983).
2. Aldén, M., Schawlow, A. L., Svanberg, S., Wendt, W., and Zhang, P.-L., *Opt. Lett.* 9:211 (1984).
3. Goldsmith, J. E. M., *Opt. Lett.* 10:116 (1985).

4. Salmon, J. T., and Laurendeau, N. M., *Opt. Lett.* 11:419 (1986).
5. Aldén, M., Edner, H., Grafström, P., and Svanberg S., *Opt. Comm.* 42:244 (1982).
6. Miziolek, A. W., and Dewilde, M. A., *Opt. Lett.* 9:390 (1984).
7. Goldsmith, J. E. M., *Opt. Lett.* 7:437 (1982).
8. Tjossem, P. J. H., and Cool, T. A., *Chem. Phys. Lett.* 100:479 (1983).
9. Goldsmith, J. E. M., *Twentieth Symposium (International) on Combustion,* The Combustion Institute, 1984, p. 1331.
10. Goldsmith, J. E. M., *J. Chem. Phys.* 78:1610 (1983).
11. Aldén, M., Hertz, H. M., Svanberg, S., and Wallin, S., *Appl. Opt.* 23:3255 (1984).
12. Goldsmith, J. E. M., and Anderson, R. J. M., *Appl. Opt.* 24:607 (1985).
13. Goldsmith, J. E. M., *Opt. Lett.* 11:416 (1986).
14. Meier, U., Kohse-Höinghaus, K., and Just, Th. *Chem. Phys. Lett.* 126:567 (1986).
15. Kohse-Höinghaus, K., Kelm, S., Meier, U., Bittner, J., and Just, Th., Proceedings of the Second Workshop of Modelling of Chemical Reaction Systems, Heidelberg, August 11-15, 1986 (to appear).
16. Meier, U., Grotheer, H.-H., and Just, Th., *Chem Phys. Lett.* 106:97 (1984).
17. Kohse-Höinghaus, K., Heidenreich, R., and Just, Th., *Twentieth Symposium (International) on Combustion,* The Combustion Institute, 1984, p. 1177.
18. Kohse-Höinghaus, K., Koczar, P., and Just, Th., *Twenty-First Symposium (International) on Combustion,* The Combustion Institute, 1986, (in press).
19. Bischel, W. K., Perry, B. E., and Crosley, D. R., *Appl. Opt.* 21:1419 (1982).
20. Bokor, J., Freeman, R. R., White, J. C., and Storz, R. H., *Phys. Rev.* A24:612 (1981).
21. Wiese, W. L., Smith, W. M., and Glennon, B. M., *Atomic Transition probabilities,* NSRDS NBS4, National Bureau of Standards, Washington, 1966.
22. See, e.g., Unsöld, A., *Physik der Sternatmosphären,* Springer, Berlin, 1955.
23. Lucht, R. P., Sweeney, D. W., and Laurendeau, N. R., *Combust. Flame* 50:189 (1980).
24. Bennett, K., and Byer, R L., *Appl. Opt.* 19:2408 (1980).
25. Warnatz, J., *Ber. Bunsenges, Phys. Chem.* 82:834 (1978).
26. Frank, P., and Just, Th., *Ber. Bunsenges. Phys. Chem.* 89:181 (1985).

Received 6 April 1987; revised 11 June 1987